Chapter 2
Linear Accelerators

Before we address the physics of beam dynamics in accelerators it seems appropriate to discuss briefly various methods of particle acceleration as they have been developed over the years. It would, however, exceed the purpose of this text to discuss all variations in detail. Fortunately, extensive literature is available on a large variety of different accelerators and therefore only fundamental principles of particle acceleration shall be discussed here. A valuable source of information for more detailed information on the historical development of particle accelerators is Livingston's collection of early publications on accelerator developments [8].

The development of charged-particle accelerators has progressed along double paths which by the appearance of particle trajectories are distinguished as linear accelerators and circular accelerators. Particles in linear accelerators travel on a straight line and pass only once through the accelerator structure while in a circular accelerator they follow a closed orbit periodically for many revolutions accumulating energy at every passage of the accelerating structure.

2.1 Principles of Linear Accelerators

No fundamental advantage or disadvantage can be claimed for one or the other class of accelerators. It is mostly the particular application and sometimes the available technology that determines the choice between both classes. Both types have been invented and developed throughout the twentieth century, and continue to be improved and optimized as associated technologies advance. In this chapter we will concentrate on linear accelerators and postpone the discussion on circular accelerators to the next chapter. In linear accelerators the particles are accelerated by definition along a straight path by either electrostatic fields or microwave fields.

2.1.1 Charged Particles in Electric Fields

In accelerator physics all forces on charged particles originate from electromagnetic
fields. For particle acceleration we consider only the electric-field term of the
Lorentz force. The nature of the electric field can be static, pulsed, generated
by a time varying magnetic field or a microwave field. Both the electric and
magnetic fields are connected by Maxwell's equations. Such fields are generated
by appropriate sources hooked up to an accelerating section which, in the case of
electro-static fields, consists of just two electrodes with the particle source at the
potential of one electrode and a hole in the center of the other electrode to let the
accelerated particles pass through. Special resonant cavities are used as accelerating
sections with two holes on the axis of the cavity to let the beam pass through. Either
field can be represented by the plane wave equation

$$\mathbf{E}(\psi) = \mathbf{E}_0 \, \mathrm{e}^{\mathrm{i}\,(\omega t - ks)} = \mathbf{E}_0 \mathrm{e}^{\mathrm{i}\psi}, \tag{2.1}$$

where ω is the frequency and k the wave number including the case of static fields
with $\omega = 0$ and $k = 0$. The Lorentz force acting on an electric charge is

$$\mathbf{F}_{\mathrm{L}} = \frac{\mathrm{d}}{\mathrm{d}t} mc\gamma\boldsymbol{\beta} = e\mathbf{E}(\psi) \tag{2.2}$$

and the equation of motion for particles under this force is

$$\frac{\mathrm{d}}{\mathrm{d}t} mc\gamma\boldsymbol{\beta} = e\mathbf{E}(\psi). \tag{2.3}$$

Integration of (2.3) results in an expression for the momentum gain of the particle

$$\Delta p = mc\,(\gamma\beta - \gamma_0\beta_0) = e \int \mathbf{E}(\psi)\,\mathrm{d}t\,, \tag{2.4}$$

where $mc\gamma_0\beta_0$ is the initial momentum of the particle. Generally, it is somewhat
complicated to perform a time integration which requires the tracking of particles
though the accelerating cavity. To simplify the calculation, we look for the gain in
kinetic energy which reduces (2.4) to a spatial integration of the electric field in the
accelerating cavity. This integral is a property of the cavity and is independent of
particle motion. With $\beta \, \Delta cp = \Delta E_{\mathrm{kin}}$ the energy gain for particles passing through
the accelerating section is

$$\Delta E_{\mathrm{kin}} = e \int_{L_{\mathrm{cy}}} \mathbf{E}(\psi)\,\mathrm{d}\mathbf{s}\,, \tag{2.5}$$

where L_{cy} is the length of the accelerating section.

The effectiveness of acceleration in a microwave field depends greatly on the phase relationship of the field with the particle motion. For successful particle acceleration we expect therefore the need to meet specific synchronicity conditions to ensure acceleration.

2.1.2   Electrostatic Accelerators

In electrostatic accelerators the potential difference between two electrodes is used for particle acceleration as shown in Fig. 2.1. The most simple such arrangement has been used now for almost two centuries in glow discharge tubes for fundamental research on the nature of plasmas, as light sources or as objects of aesthetic interest due to colorful phenomena in such tubes. In another, more modern application electrons are accelerated in an x-ray tube by high electrostatic fields and produce after striking a metal target intense x-rays used in medicine and industry.

The voltages that can be achieved by straight voltage transformation and rectification are quite limited by electrical breakdown effects to a few 10,000 V/cm. More sophisticated methods of producing high voltages therefore have been developed to reach potential differences of up to several million volts.

To distribute evenly the electric fields of high potential differences a series of irises are distributed along the acceleration column and separated by appropriate resistors to break down the high voltage into smaller steps between the irises. As an added benefit we also gain focusing of the particle beam as will be discussed later in this chapter.

A variety of techniques to obtain high voltages have been developed and applied to particle acceleration with more or less success. We will discus briefly a few of theses techniques because they are still used.

Fig. 2.1 Principle of electrostatic accelerators
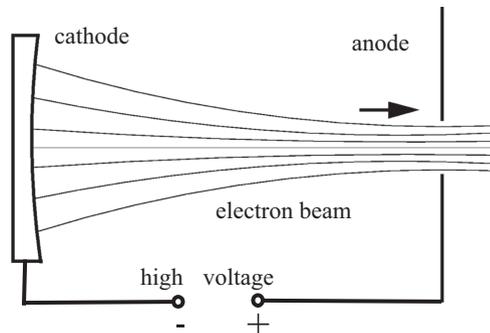
Cascade Generators

The basic method implemented in the cascade generator is that of a voltage multiplier circuit which has been proposed by Greinacher [5] in 1914 and Schenkel [10] in 1919 which allows to achieve a multiplication of the voltage across the plates of a capacitor. A set of capacitors are charged through appropriately placed diodes from an alternating current source (Fig. 2.2) in such a way that during the positive half wave, half the capacitors are charged to a positive voltage and during the negative half wave, the other half of the capacitors are charged to a negative voltage thus providing twice the maximum ac voltage. By arranging $2N$ capacitors in this way the charging voltage can be multiplied by the factor N.

While there is no fundamental limit to the total voltage, high voltage break down will impose a technical limit on the maximum achievable voltage. Based on this method Cockcroft and Walton [3] developed appropriate high-voltage techniques and built the first high energy particle accelerator reaching voltages as high as several million Volt. Applying the high voltage to a beam of protons they were able for the first time to initiate through artificially accelerated protons a nuclear reaction. In this case it was the conversion of a Lithium nucleus into two helium nuclei, in the reaction

$$p + Li \rightarrow 2He \,. \tag{2.6}$$

Such Cockcroft-Walton accelerators turned out to be very efficient and are still used as the first step in modern proton accelerator systems. Obviously with this kind of voltage generation it is not possible anymore to produce a continuous stream of particles. Because of the switching process, there is a time to charge the capacitors followed by a time to apply the multiplied voltage to particle acceleration. As a consequence, we observe a pulsed particle beam from a Cockroft-Walton accelerator.
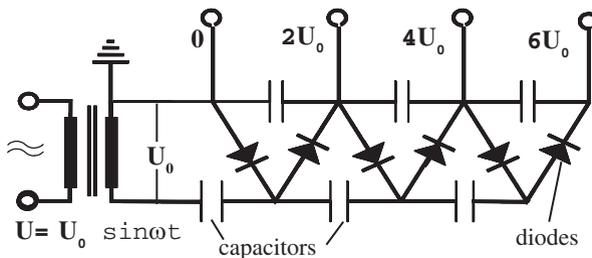

Fig. 2.2 Cascade generator (schematic)

Van de Graaff Accelerator

Much higher voltages can be reached with a Van de Graaff accelerator [12]. Here, electric charge is extracted by field emission from a pointed metal electrode and sprayed onto an isolated endless belt. This belt is moved by motor action to carry the charge to the inside of a hollow sphere, where the charge is stripped off again by reverse field emission onto a pointed metal electrode which is connected to the inside of the sphere. The principle of this electrostatic generator is shown in Fig. 2.3. Electrical charges in a metallic conductor collect on the outside and it is therefore possible to continuously accumulate electrical charge by deposition to the inside surface of a hollow metallic sphere. If the whole system is placed into a high pressure vessel filled with an electrically inert gas like Freon or SF_6, voltages as high as 20 million volts can be reached.

The high voltage can be used to accelerate electrons as well as protons or ions. In the latter two cases more than double the accelerating voltage can be achieved in a Tandem Van de Graaff accelerator. If a proton beam must be accelerated, the accelerating process would start with negatively charged hydrogen ions H^- from a plasma discharge tube which are then accelerated say from ground potential to the full Van de Graaff voltage $+V$. At that point the two electrons of the negative hydrogen ion are stripped away by a thin foil or gas curtain resulting by charge exchange in positively charged protons which can be further accelerated between the potential $+V$ and ground potential to a total kinetic energy $E_{kin} = e2V$.
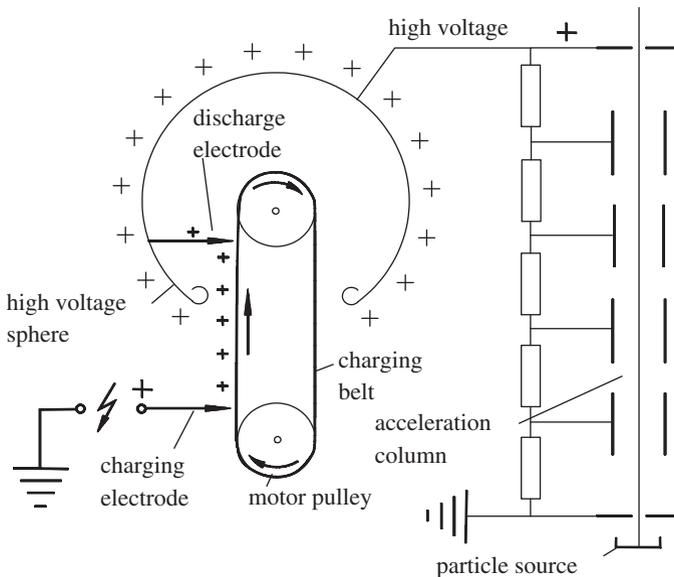

Fig. 2.3 Van de Graaff accelerator (schematic)

High electrostatic voltages from a Van de Graaff generator cannot be applied directly to just two electrodes as shown in Fig. 2.1. Because of the great distance between the electrodes necessary to avoid voltage break down the fields would not be distributed uniformly along the axis of the acceleration column. Therefore, the voltage is applied to a series of resistors connected to iris electrodes which allow a uniform distribution of the electrical field along the acceleration column as shown in Fig. 2.3. A more detailed review of the development of electro-static high voltage generators can be found in [13].

2.2   Electric Field Components

In our discussion we concentrate first on the interaction of particles with electro-static fields. Such field components function both as focusing and acceleration devices. Electro-static fields are commonly employed for low energy, non-relativistic particles. As was discussed earlier, magnetic devices are most effective at high energies when particle velocities are close to the speed of light. At lower velocities, magnetic fields loose their efficiency and are often replaced by more economic electric field devices and at very low energies electric fields are used almost exclusively.

2.2.1   Electrostatic Deflectors

The electric field $\boldsymbol{E}$ between two parallel metallic electrodes is uniform and can be used to deflect a particle beam. To get a uniform field, we generate equipotential surfaces by placing metallic electrodes at, for example, $x = \pm G =$ const. and applying a voltage difference V between the electrodes. The Lorentz force of the electric field on a charged particle is by virtue of d'Alembert's principle equal to the centrifugal force and is for a horizontal deflection

$$eZ\boldsymbol{E}_x = \frac{\gamma Amc^2\beta^2}{\rho} \ . \tag{2.7}$$

Here we have assumed that the electric field is parallel to the vector from the particle to the center of curvature. That is true for parallel plates which are curved to follow the curvature or almost true for straight parallel plates if the deflection angle is very small. Solving for the curvature, we get

$$\frac{1}{\rho} = \frac{eZ\boldsymbol{E}_x}{\gamma Amc^2\beta^2} = \frac{eZ}{2G}\frac{V}{E_{\text{kin}}}\frac{\gamma}{\gamma+1}, \tag{2.8}$$

where $2G$ is the distance and V the voltage between the electrodes. We kept here the relativistic notation to cover the rare use of electrostatic fields on high energy beams for small deflections which cannot be done by magnetic fields. For nonrelativistic particles, (2.8) reduces to $\frac{1}{\rho} = \frac{eZE_x}{Amv^2}$ or in case of an ion beam with charge multiplicity Z and kinetic energy per nucleon $E_{kin} = \frac{1}{2}mv^2$

$$\frac{1}{\rho} \left(\text{m}^{-1}\right) = \frac{eZE_x \,(\text{V/m})}{2AE_{kin}\,(\text{eV})} \,.$$ (2.9)

where $E_x = V/(2G)$ is the electric field between the electrodes.

2.2.2 Electrostatic Focusing Devices

The most simple electro-static device with focusing properties is an iris electrode on some potential and coaxial with the path of a charged particle beam as shown in Fig. 2.4.

To determine the field configuration and focusing properties, we note that the electric potential distribution $V(r, z)$ in the vicinity of the iris is rotationally symmetric and expanding into a Taylor series about $r = 0$ this symmetry requires all odd terms of the expansion to vanish.

$$V(r, z) = V_0(z) + \frac{1}{2}\ddot{V}_0(z)\,r^2 + \frac{1}{24}\frac{\partial^4 V_0(z)}{\partial r^4}r^4 + \cdots .$$ (2.10)

Derivatives with respect to r are indicated with a dot and derivatives with respect to z with a prime. To be a real potential solution (2.10) must also be a solution of the Laplace equation

$$\Delta V = \frac{\partial^2 V}{\partial r^2} + \frac{1}{r}\frac{\partial V}{\partial r} + \frac{\partial^2 V}{\partial z^2} = 0 \,.$$ (2.11)
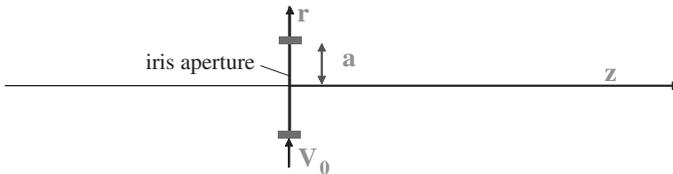

Fig. 2.4 Iris electrode

Inserting (2.10) into (2.11) results in

$$0 = \ddot{V}_0 + \frac{1}{2}\frac{\partial^4 V_0}{\partial r^4}r^2 + \frac{1}{2}\dddot{V}_0 r + \ddot{V}_0 + \frac{1}{6}\frac{\partial^4 V_0}{\partial r^4}r^2 + V_0'' + \frac{1}{2}\ddot{V}_0'' r^2 + \cdots , \qquad (2.12)$$

where the coefficients of each term r^n must be equal to zero separately to give $2\ddot{V}_0 + V_0'' = 0$, $\dddot{V}_0 = 0$ and $\frac{2}{3}\frac{\partial^4 V_0}{\partial r^4} + \frac{1}{2}\ddot{V}_0'' = 0$. Using these relations, we set $\frac{\partial^4 V_0}{\partial r^4} = \frac{3}{8}\frac{\partial^4 V_0}{\partial z^4}$ and the potential function is

$$V(r, z) = V_0(z) - \frac{1}{4}V_0''(z)r^2 + \frac{1}{64}\frac{\partial^4 V_0(z)}{\partial z^4}r^4 + \cdots . \qquad (2.13)$$

The on-axis ($r = 0$) field component is

$$E_z = -V_0'(z) , \qquad (2.14)$$

and from $\nabla E = 0$ or $\frac{\partial E_z}{\partial z} = -\frac{1}{r}\frac{\partial}{\partial r}(rE_r)$, we get by integration

$$E_r = -\frac{r}{2}\frac{\partial E_z}{\partial z} = \tfrac{1}{2}V_0''(z) r . \qquad (2.15)$$

Knowing the field components, we can derive the focusing properties by integrating the radial equation of motion $m\ddot{r} = mv^2 r'' = qE_r$, where v and q are the particle velocity and charge, respectively. We use Fig. 2.5 to define the integration

$$r_2' - r_1' = \frac{q}{mv^2}\int_{z_1}^{z_2} E_r \, dz = -\frac{q}{2mv^2}\int_{z_1}^{z_2} r\frac{\partial E_r}{\partial z} \, dz$$

and solve in thin lens approximation ($r = \text{cost}, v = \text{cost}$)

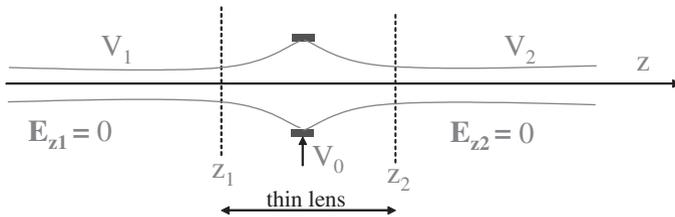$$r_2' - r_1' = -\frac{q\,r_1}{2mv^2}(E_2 - E_1) . \qquad (2.16)$$

Fig. 2.5   Focusing by an iris electrode

With $\frac{1}{2}mv^2 = qV_0$ and setting $E = -V'$, (2.16) becomes $r'_2 - r'_1 = \frac{r_1}{4}\frac{V'_2 - V'_1}{V_0}$ and the focal length of the iris electrode is

$$\frac{1}{f} = \frac{V'_2 - V'_1}{4V_0} \tag{2.17}$$

and the transformation matrix is finally

$$\mathcal{M}_{\text{iris}} = \begin{pmatrix} 1 & 0 \\ \frac{V'_2 - V'_1}{V_0} & 1 \end{pmatrix} . \tag{2.18}$$

From the transformation matrix or focal length it is obvious that there is no focusing for a symmetric iris electrode where $V'_2 = V'_1$. On the other hand, an asymmetric potential is not possible without additional electrodes. We investigate therefore the properties of an iris doublet.

2.2.3 Iris Doublet

We now investigate the particle dynamics for an iris doublet as shown in Fig. 2.6. Between both electrodes a distance d apart, the potential varies linearly from V_1 to V_2. The doublet has three active parts, two iris electrodes and the drift space between them. The transformation matrices for both iris electrodes are

$$\mathcal{M}_1 = \begin{pmatrix} 1 & 0 \\ \frac{V_2 - V_1}{4dV_1} & 1 \end{pmatrix} \qquad \text{and} \qquad \mathcal{M}_2 = \begin{pmatrix} 1 & 0 \\ \frac{V_2 - V_1}{4dV_2} & 1 \end{pmatrix} . \tag{2.19}$$

The transformation matrix for the drift space between the electrodes can be derived from the particle trajectory

$$r(z) = r_1 + \int_0^z r'(\bar{z}) \, d\bar{z} = r_1 + \int_0^z \frac{r' p_1}{p_1 + \Delta p(\bar{z})} \, d\bar{z} . \tag{2.20}$$
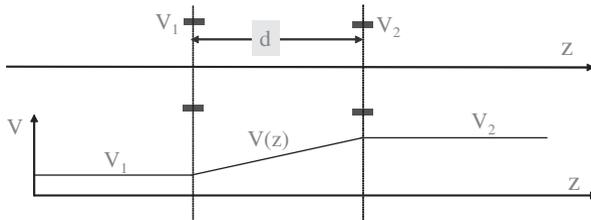

Fig. 2.6 Focusing by an iris doublet

The particle momentum varies between the electrodes from $p_1 = \sqrt{2mE_{\text{kin}}}$ to $p_1 + \Delta p(\bar{z}) = \sqrt{2m\left(E_{\text{kin}} + q\frac{V_2-V_1}{d}z\right)}$ and the integral in (2.20) becomes

$$\int_0^d \frac{\text{d}\bar{z}}{\sqrt{1+\frac{V_2-V_1}{E_{\text{kin}}d}z}} = \frac{2E_{\text{kin}}d}{q\,(V_2-V_1)}\sqrt{1+q\frac{V_2-V_1}{E_{\text{kin}}d}z}\,\Bigg|_0^d = \frac{2d\sqrt{V_1}}{\sqrt{V_2}+\sqrt{V_1}}.$$

(2.21)

The particle trajectory at the location of the second electrode is $r(d) = r_2 = r_1 + \frac{2d\sqrt{V_1}}{\sqrt{V_2}+\sqrt{V_1}}r_1'$ and its derivative $r_2' = r_1'\sqrt{V_1}/\sqrt{V_2}$ from which we can deduce the transformation matrix

$$\mathcal{M}_{\text{d}} = \begin{pmatrix} 1 & \frac{2d\sqrt{V_1}}{\sqrt{V_2}+\sqrt{V_1}} \\ 0 & \frac{\sqrt{V_1}}{\sqrt{V_2}} \end{pmatrix}.$$

(2.22)

We may now collect all parts and get the transformation matrix for the iris doublet

$$\mathcal{M}_{\text{db}} = \mathcal{M}_2 \mathcal{M}_{\text{d}} \mathcal{M}_1 = \begin{pmatrix} \frac{1}{2}(R+1) & \frac{2d}{1+R} \\ \frac{(R^2-1)(3R+1)}{8dR^2} & \frac{3R-1}{2R^2} \end{pmatrix},$$

(2.23)

where $R = \sqrt{V_2}/\sqrt{V_1}$. Unfortunately, this doublet is still not very convenient since it still changes the energy of the particle as indicated by the fact that the determinant $\det(\mathcal{M}_{\text{db}}) = 1/R$. As indicated earlier this focusing device is also an accelerating structure. Any two adjacent irises along a high voltage accelerating structure act like a focusing device while accelerating particles.

2.2.4   Einzellens

To obtain a focusing device that does not change the particle energy, we combine two doublets to form a symmetric triplet as shown in Fig. 2.7. The transformation
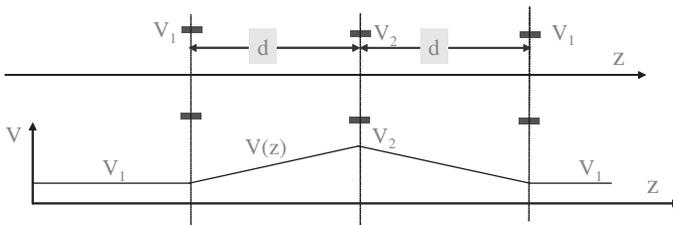

Fig. 2.7   Structure of an Einzellens

matrix for such an Einzellens is then the product of two symmetric doublets

$$\mathcal{M}_{el} = \mathcal{M}_{2d}\left(V_2, V_1\right)\mathcal{M}_{1d}\left(V_1, V_2\right) = \begin{pmatrix} m_{11} & m_{12} \\ m_{21} & m_{22} \end{pmatrix}, \tag{2.24}$$

where

$$\begin{array}{ll} m_{11} = 4 - \frac{3R}{2} - \frac{3}{2R}, & m_{12} = \frac{2d}{R}\frac{3R-1}{1+R}, \\ m_{21} = \frac{3\left(R^2-1\right)(1-R)(3-R)}{8dR}, & m_{22} = 4 - \frac{3}{2R} - \frac{3R}{2}, \end{array} \tag{2.25}$$

and $R = \frac{\sqrt{V_2}}{\sqrt{V_1}} = \sqrt{1 + \frac{V}{V_1}} = \sqrt{1 + \frac{qV}{E_{kin}}}$. The Einzellens displays some peculiar focusing properties depending on the potentials involved compared with the particle's kinetic energy. The focal length of the Einzellens is

$$\frac{1}{f} = \frac{3}{8dR}\left(1 - R^2\right)(R - 1)(3 - R). \tag{2.26}$$

Varying the potential V, we obtain varying focusing conditions as summarized in the following table and plotted as a function of R in Fig. 2.8.

The results of focusing properties in an Einzellens are compiled in the following table. Depending on the chosen voltage the Einzel-lens can be focusing or defocusing.

V	$V < -V_1$	$-V_1 < V < 0$	$0 < V < 8V_1$	$V > 8V_1$
R	imaginary	$0 < R < 1$	$1 < R < 3$	$R > 3$
$1/f$	no solution	> 0	> 0	< 0
	n/a	focusing	focusing	de-focusing

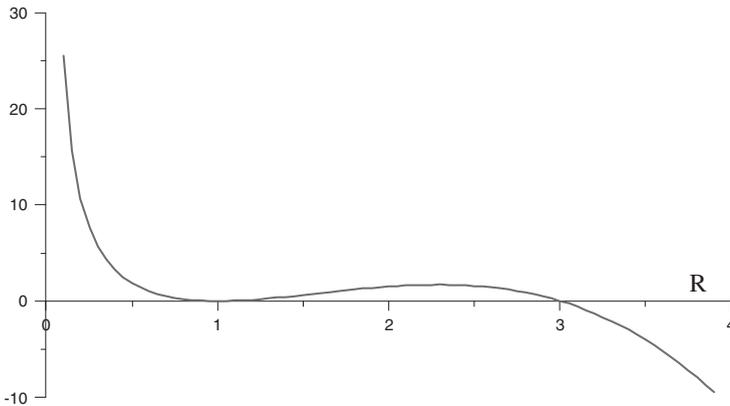**Fig. 2.8** Focusing $8d/3f$ from (2.26) in an Einzellens as a function of R

The practical focusing regime is limited to $0 < R < 1$. For $1 < R < 3$ the focusing is very weak and for $R > 3$ the Einzellens is defocusing.

2.3   Acceleration by rf Fields

The most successful acceleration of particles is based on the use of rf fields for which by now powerful sources exist. Very high accelerating voltages can be achieved in resonant rf cavities far exceeding those obtainable in electrostatic accelerators of similar dimensions. Particle acceleration in linear accelerators as well as in circular accelerators are based on the use of rf fields and we will in the following sections and in the next chapter discuss the principles of the more important types of particle accelerators.

2.3.1   Basic Principle of Microwave Linear Accelerators

The principle of the linear accelerator based on microwave fields and drift tubes was proposed by Ising [6] and Wideroe. [14] The accelerator consists of a series of coaxial metallic tubes where the accelerating field is generated in gaps between adjacent tubes. In this method particles are accelerated by repeated application of rf fields. Wideroe constructed such an accelerator and was able to accelerate potassium ions up to 50 keV.

While the principle is simple, the realization requires specific conditions to ensure that the particles are exposed to only accelerating rf fields. The particles travel through the metallic tubes while the field is not suitable for acceleration as shown in Fig. 2.9. The tubes shield the particles from external rf fields and the length of the tube segments are chosen such that the particles reach the gap between two successive tubes only when the rf field is accelerating.

Synchronicity Condition

For efficient acceleration the motion of the particles must be synchronized with the rf fields in the accelerating sections. The distance between the center of two adjacent gaps must be equal to the travel time of the particles from one gap to the next. The length of the drift tubes are chosen such that the particles travel for most of the rf period in the field free interior and emerge in a gap to the next drift tube at a moment the field is accelerating. The length of the shielding tubes is therefore almost as long as it take the particles to travel in a full rf period. In this case, we have synchronism between particle motion and rf field and the length of the ith drift tube/section is

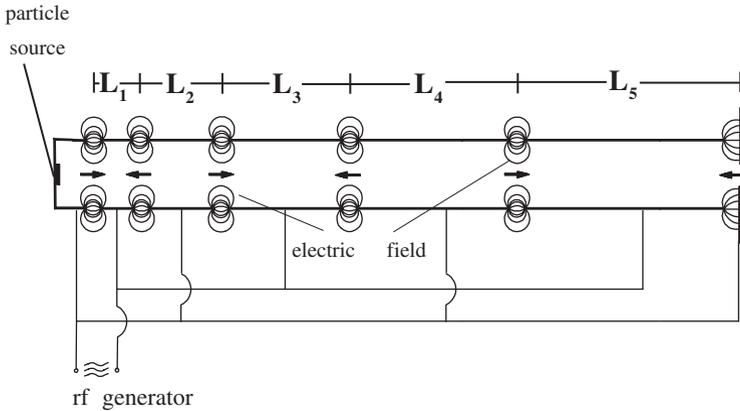$$L_i \approx v_i \, T_{\rm rf} \,, \tag{2.27}$$

Fig. 2.9 Wideroe linac structure (schematic)

where v_i is the velocity of the particles in the ith section and T_{rf} the rf period.

Stimulated by the successful acceleration of potassium ions by Wideroe, a group led by Sloan and Lawrence at Berkeley were able to build a 50 kW rf generator oscillating at 10 MHz and delivering a gap voltage of 42 kV. Applying this to 30 acceleration tubes they were able to accelerate mercury ions to a total kinetic energy of 1.26 MeV [11].

In the 1920s when this principle was developed it was difficult to build high frequency generators at significant power. In 1928 rf generators were available only up to about 7 MHz and numerical evaluation of (2.27) shows that this principle was useful only for rather slow particles like low energy protons and ions. The drift tubes can become very long for low rf frequencies and particles traveling with, for example, half the speed of light would require a drift tube length of 10.7 m at 7 MHz. Such long drift tubes add up quickly to a very long accelerators before the particles approach the speed of light. To reduce the length of the tubes, higher frequencies are required.

Further progress in the development of rf linear accelerators therefore depended greatly on the development of rf equipment at high frequency which happened during World War II in connection with the development of radar systems. In 1937, Hansen and the Varian brothers invented the klystron at Stanford. Soon the feasibility of high power klystrons had been established [2] which to this date is one of the most efficient rf amplifiers available. The first klystron was developed for 3,000 MHz which is still the preferred frequency for high energy electron linear accelerators. The klystron principle is economically feasible from about 100 MHz to more than 10 GHz. With such a wide range of high frequencies available, the principle of rf acceleration in linear accelerators has gained quick and continued prominence for the acceleration of protons as well as electrons.

Going to higher frequencies, however, the capacitive nature of the Wideroe structure becomes very lossy due to electromagnetic radiation. To overcome this
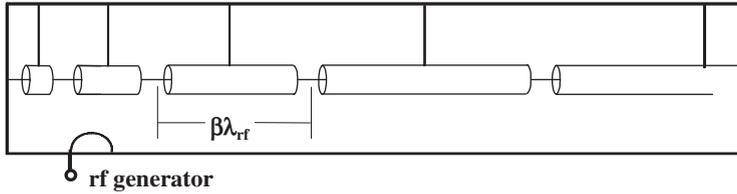
Fig. 2.10   Alvarez linac structure (schematic)

difficulty, Alvarez [1] proposed to enclose the gaps between the tubes by metallic cavities (Fig. 2.10). The acceleration section would now be composed of a series of tubes forming, together with the outer enclosure, a resonant cavity.

This Alvarez structure is still the preferred preaccelerator to accelerate protons and ions from a few hundred keV out of a Cockroft-Walton electrostatic generator to a few hundred MeV for injection into a booster synchrotron. Because of the lower velocity of protons and ions at up to a few hundred MeV the operating frequency for proton linacs is generally around 200 MHz.

Radio frequencies of 3,000 MHz and higher are desired for electron acceleration. In Chap. 18.4 we will discuss in more detail the basic features and scaling of high frequency accelerating structures to give the interested reader the tools to understand the scaling and limitations of basic linear accelerator physics. For more detailed discussion of rf aspects in linear electron accelerators, the reader is referred to the literature [4, 7, 9].

Problems

2.1 (S). Derive the geometry of electrodes for a horizontally deflecting electric dipole with an aperture radius of 2 cm which is able to deflect an electron beam with a kinetic energy of 10 MeV by 10 mrad. The dipole be 0.1 m long. What is the electric field required between the electrodes?

2.2 (S). Calculate the minimum power rating for the motor driving the charging belt of a Van de Graaff accelerator while producing a charge current of 100 mA at 5 MV.

2.3 (S). Calculate the length for the first four drift tubes of a Wideroe linac for the following parameters: starting kinetic energy is 100 keV, the energy gain per gap is 1 MeV, and the microwave frequency 7 MHz. Assume the gaps to be of zero length for simplicity. Perform the calculations for both electrons and singly charged potassium ions (A_K = 39.0983 amu $\approx$ 39; 1 amu $\approx$ 1 GeV) and compare the results.

References

1. L.W. Alvarez, Phys. Rev. **70**, 799 (1946)
2. M. Chodorow, E.L. Ginzton, I.R. Neilsen, S. Sonkin, Proc. IRE **41**, 1584 (1953)
3. J.D. Cockcroft, E.T.S. Walton, Proc. Roy. Soc A **136**, 619 (1932)
4. E.L. Ginzton, W.W. Hansen, W.R. Kennedy, Rev. Sci. Inst. **19**, 89 (1948)
5. H. Greinacher, Z. Physik **4**, 195 (1921)
6. G. Ising, Arkiv för Matematik, Astronomi och Fysik **18**, 1 (1924)
7. P. Lapostolle, A. Septier (eds.), *Linear Accelerators* (North-Holland, Amsterdam, 1970)
8. M.S. Livingston (ed.), *The Development of High-Energy Accelerators* (Dover, New York, 1966)
9. R. Neal (ed.), *The 2 Mile Linear Accelerator* (Benjamin, New York, 1968)
10. M. Schenkel, Elektrotech. Z. **40**, 333 (1919)
11. D.H. Sloan, E.O. Lawrence, Phys. Rev. **38**, 2021 (1931)
12. R.J. Van de Graaff, Phys. Rev. **38**, 1919 (1931)
13. R.J. Van de Graaff, J.G. Trump, W.W. Buechner, Rep. Prog. Phys. **11**, 1 (1948)
14. R. Wideroe, Archiev für Elektrotechnik **21**, 387 (1928)